THE JOURNAL OF PHYSICAL CHEMISTRY Letters

Perspective

Cite This: J. Phys. Chem. Lett. 2018, 9, 3253−3263

pubs.acs.org/JPCL

Capturing Structural Snapshots during Photochemical Reactions with Ultrafast Raman Spectroscopy: From Materials Transformation to Biosensor Responses

Chong Fang,* Longteng Tang, Breland G. Oscar, and Cheng Chen

Department of Chemistry, Oregon State University, 153 Gilbert Hall, Corvallis, Oregon 97331, United States

ABSTRACT: Chemistry studies the composition, structure, properties, and transformation of matter. A mechanistic understanding of the pertinent processes is required to translate fundamental knowledge into practical applications. The current development of ultrafast Raman as a powerful time-resolved vibrational technique, particularly femtosecond stimulated Raman spectroscopy (FSRS), has shed light on the structure−energy−function relationships of various photosensitive systems. This Perspective reviews recent work incorporating optical innovations, including the broad-band up-converted multicolor array (BUMA) into a tunable FSRS setup, and demonstrates its resolving power to watch metal speciation and photolysis, leading to high-quality thin films, and fluorescence modulation of chimeric protein biosensors for calcium ion imaging. We discuss advantages of performing FSRS in the mixed time−frequency domain and present strategies to delineate mechanisms by tracking low-frequency modes and systematically modifying chemical structures with specific functional groups. These unique insights at the chemical-bond level have started to enable the rational design and precise control of functional molecular machines in optical, materials, energy, and life sciences.

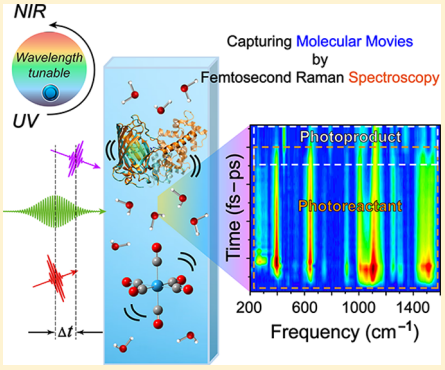

Downloaded via UNIV OF SUSSEX on July 24, 2018 at 10:59:31 (UTC).
See https://pubs.acs.org/sharingguidelines for options on how to legitimately share published articles.

Light−matter interactions are omnipresent in nature, powering physical and chemical processes from photosynthesis, luminescence, human vision, to green chemistry.[1−9] The mechanistic understanding of such processes on intrinsic molecular time scales, starting from the photoexcitation time zero, holds fundamental importance and translational implications. Steady-state and time-resolved electronic spectroscopy have provided the absorption and emission profiles that probe the potential energy surface (PES) in the system's Hamiltonian, but nuclear motions hold the key to revealing reaction coordinates for photoinduced events such as proton transfer, isomerization, intersystem crossing, and fluorescence. A recent review on femtosecond crystallography with ultrabright electrons and X-rays highlighted the importance of resolving the far-from-equilibrium motions directing chemical processes.[10] The experimental methodology to achieve this atomic resolution could come from sophisticated ultrafast electron or X-ray sources, which are technically demanding for most of the ultrafast spectroscopy groups. Given the wide availability of commercial Ti:sapphire-based femtosecond laser systems, the broad community can benefit significantly from a generally accessible tabletop coherent optical spectroscopic setup that can fulfill the need to capture real-time nuclear motions.

> A major challenge in tracking structural dynamics of molecular systems is to increase the signal-to-noise ratio of transient species with sufficiently high spatial and temporal resolutions.

Ideally, elucidation of the highly sought-after structure−function relationships comes from a frame-by-frame visualization of molecular structure during a chemical reaction and key nuclear dynamics that could play an active role. Numerous efforts and advances have been made for molecular systems at thermal equilibrium or in the ground state, but taking vivid molecular "movies" in the electronic excited state remains a formidable challenge to experimentalists and theoreticians. A successful strategy needs to achieve sufficient spatial and temporal resolutions from the stationary to nonstationary states, improve versatility to study various systems, and gain the capability of tracking nuclear motions after photoexcitation. Such motions could arise from a proton, while the reversible or irreversible structural changes start to occur within a vibrational period and/or within the Franck−Condon (FC) region, where an intimate yet underexplored connection exists between microscopic events (e.g., proton motions, structural evolution) and the onset of macroscopic functions (e.g., photoacidity, fluorescence).[11−14]

Why Stimulated Raman? With the advance of laser technologies and imaging methodologies, Raman spectroscopy has shown great potential to sensitively collect structural information

Received: February 4, 2018
Accepted: May 25, 2018
Published: May 25, 2018

© 2018 American Chemical Society

DOI: 10.1021/acs.jpclett.8b00373
J. Phys. Chem. Lett. 2018, 9, 3253−3263

corresponding to biochemical and pathophysiological processes. Notably, stimulated Raman scattering (SRS) was used to enable the high-resolution video-rate molecular imaging in vivo by enhancing the collection of backscattered signal with increased imaging speed.[15,16] Therefore, SRS can directly benefit microscopy and spectroscopy; in this Perspective, we focus on the latter area because we have actively pushed for a deeper understanding of photochemistry along the intrinsic reaction coordinates in real time. Richard Feynman wrote in his seminal 1963 *Lectures on Physics*, "Everything that living things do can be understood in terms of the jiggling and wiggling of atoms." Spectroscopy addresses this task by exposing atomic motions frame by frame on microscopic time scales, instead of collecting holistic images of a molecule, cell, or whole animal on macroscopic time scales. The pioneering reports[17,18] before the early 2000s laid the groundwork for the femtosecond stimulated Raman spectroscopy (FSRS) method. Joint efforts from experimental and theoretical groups over the past decade[3,5,8,9,13,14,19−46] have developed FSRS into a versatile spectroscopic platform to interrogate many photosensitive systems and fill the knowledge gap between structure and function in the broad science and engineering fields.

To further improve the resolving power and utility of FSRS, we discuss our experimental strategies to improve the signal-to-noise ratio in the vibrational low-frequency region for solution samples. There has been extensive interest in revealing skeletal motions and their potential roles in facilitating a chemical reaction,[14,22,27,47] and 2D FSRS provides such a tool particularly when the fifth-order signal can be isolated or enhanced to report on vibrational anharmonicities in a multidimensional excited-state PES.[5,9,14] Ongoing experimental effort is aided by theoretical work, including the simulation of FSRS during energy flow and through conical intersections.[48,49]

Optical Innovations and Wavelength Tuning Critically Improve FSRS Capabilities. Figure 1 presents an overview of our experimental setup and recent applications in biological and energy sciences. A typical FSRS apparatus includes a femtosecond (fs) actinic pulse for photoexcitation, a narrow-band picosecond (ps) Raman pump, and a broad-band fs Raman probe, all tunable in the UV to near-IR region,[18,33,43] which enable the targeted resonance enhancement for specific molecular vibrations during a photoinduced process. The coincidence of Raman pump and probe pulses is optimized by maximizing a standard solvent signal in the ground state, while the time delay between the actinic pump and Raman probe pulses is varied as the time axis.[18,27] Engaged readers can find more technical details and application notes about the tunable FSRS setup in our laboratory[8,14,27,28,32,33,45] and in the broader field from recent comprehensive reviews.[9,43]

Through experimental investigation of a series of photosensitive molecules from organic chromophores in solution[14,27,28,33,50] to FP biosensors,[13,32,46,51] we devise a general rule to enhance excited-state Raman peaks: tuning the Raman pump to the red side of a transient electronic band. Because molecules commonly display transient electronic features of ground-state bleaching, excited-state absorption, and stimulated emission from short to long wavelengths, it is beneficial to find a less overlapped spectral region on the red side (avoiding overlap with ground-state absorption) to position the Raman pump. Tuning the Raman probe also constitutes a strategy because bluer/redder probe photons lead to the anti-Stokes/Stokes FSRS signal, respectively, which cannot be simply considered as an inverted copy of each other.[21,44,45] Different signal line

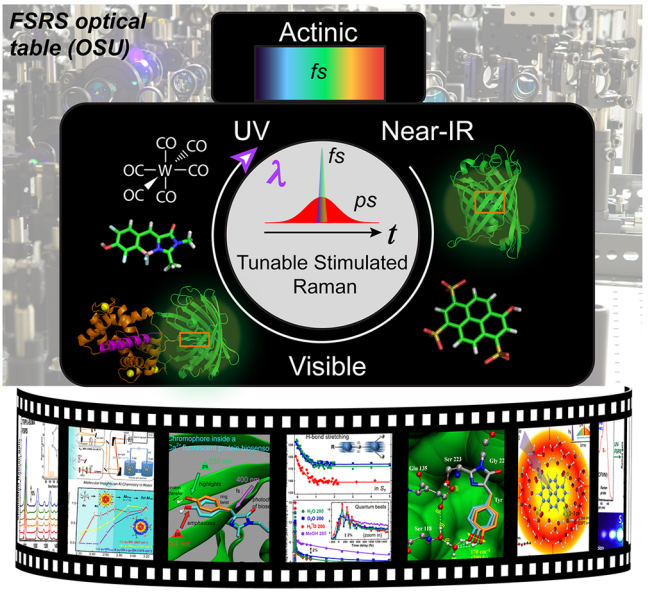

Figure 1. Tunable ultrafast Raman provides a powerful platform to elucidate structural dynamics of photosensitive molecular systems. (Upper) Our experimental apparatus consists of a sequence of fs−ps laser pulses that can be tuned to investigate a wide range of functional materials and biomolecules in action. (Lower) Representative conformational snapshots of photoacids, metal−organic complexes, fluorescent protein (FP)-based calcium biosensors, and laser dyes in solution following fs laser irradiation at various wavelengths from near-IR to UV. Film reel pictures (from left to right) with permission: Reproduced from ref 33. Copyright 2014, AIP Publishing. Adapted from ref 8. Copyright 2013, National Academy of Sciences. Reproduced from ref 51. Copyright 2016, American Chemical Society. Adapted from ref 14. Copyright 2016, Royal Society of Chemistry. Adapted from ref 32. Copyright 2014, National Academy of Sciences. Reproduced from ref 45. Copyright 2017, American Chemical Society.

Performing FSRS in the mixed time−frequency domain provides notable advantages to experimentally track transient vibrational dynamics and coupling with substantial convenience, straightforward interpretation, selective enhancement, and high fidelity.

shape, sign, and intensity dependence on the Feynman diagrams provide rich knowledge about vibronic coupling, vibrational cooling, and structural evolution.[26,45,52,53] This information unravels the multidimensional photochemical reaction coordinate in action when transient reactant and product species exhibit distinct electronic features and dynamics.[14,45]

To extend Raman probe tunability to regions near 800 or 400 nm where the laser fundamental pulse (FDP) or second-harmonic generation (SHG) pulse residual overwhelms the nascent supercontinuum white light (SCWL), we developed a broad-band up-converted multicolor array (BUMA) methodology to obtain a background-free Raman probe that can be conveniently tuned by changing the crossing angle or time delay between the two incident beams (Figure 2a,c).[31,34,54,55]

DOI: 10.1021/acs.jpclett.8b00373
J. Phys. Chem. Lett. 2018, 9, 3253−3263

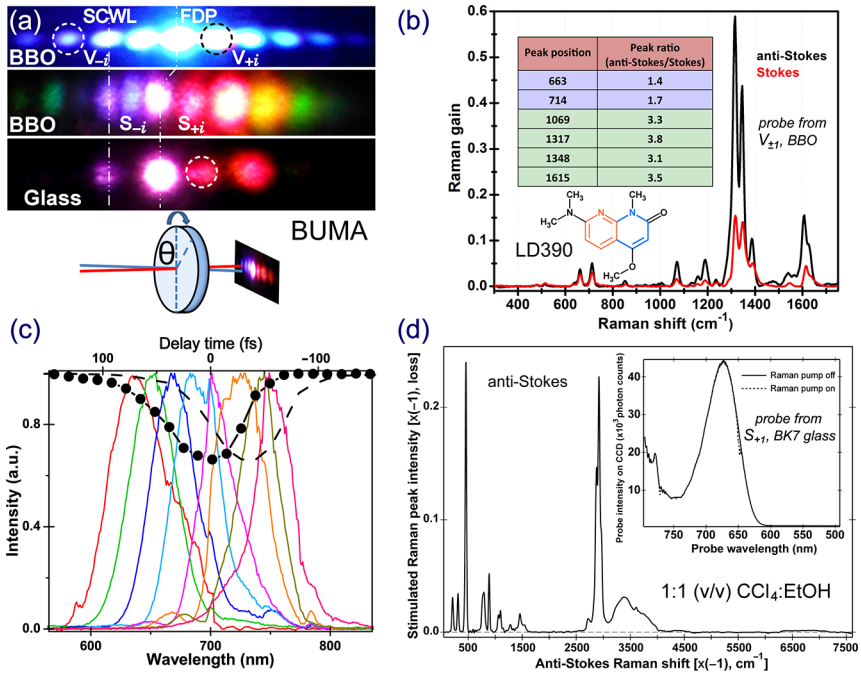

Figure 2. Optical innovations advance tunable FSRS methodology. (a) The cascaded four-wave mixing effect generates the BUMA sidebands. Adapted from ref 54. Copyright 2013, Optical Society of America. (b) Ground-state Stokes and anti-Stokes FSRS signals of laser dye LD390 in methanol collected with a ~402 nm Raman pump from SHBC and the UV-BUMA $V_{\pm1}$ sidebands, as shown in (a). Reproduced from ref 34. Copyright 2015, the authors. (c) Normalized S_{+1} spectra from BBO at various time delays between the two incident pulses FDP and SCWL, while the integrated signal intensity is plotted in black dots against the time axis on the top. Reproduced from ref 54. (d) Ground-state anti-Stokes FSRS of a mixed solvent standard spanning a spectral range over 4000 cm^{-1}, achieved with an ~800 nm Raman pump and the BUMA S_{+1} sideband from glass, as in (a). Reproduced from ref 31. Copyright 2013, AIP Publishing.

Such wavelength tuning is reminiscent of a noncollinear optical parametric amplifier (NOPA),[33,55] which is also used to generate the tunable fs actinic pump and ps Raman pump in FSRS. Besides amorphous BK7 glass with common $\chi^{(3)}$ properties among all optical materials, a thin quadratic medium such as a BBO crystal provides additional phase-matching conditions due to a large $\chi^{(2)}$ coefficient; therefore, SHG-assisted BUMA sidebands in the UV region can be generated. Together with a narrow-band Raman pump at 800 nm from a home-built spectral filter[27,28,43] or at 400 nm from a home-built second harmonic bandwidth compressor (SHBC),[33,34] we collected high-quality Stokes and anti-Stokes FSRS data of organic solvent and highly fluorescent dyes in the electronic ground (Figure 2b,d) and excited states from the UV to near-IR region.[31,34,50,56] The BUMA technology thus expands the resolving power of FSRS across a broad spectral range.

A robust baseline drawing procedure and more complete theoretical description of FSRS experimental data stemming from molecular events, particularly on or near resonance conditions, will further empower the ultrafast Raman methodology.

With these optical advances, a number of metal-containing solution precursors to generate high-quality metal oxide thin films can be studied to decipher the metal transformation mechanism at the molecular level. We first studied the pH-dependent formation of *flat* $[Al_{13}(\mu_3\text{-}OH)_6(\mu_2\text{-}OH)_{18}(H_2O)_{24}]^{15+}$ nanoclusters in water with ground-state FSRS from ~350 to 1400 cm^{-1}. The Al−O vibrational modes below 600 cm^{-1} showed a reaction plateau between pH = 2.45 and 2.70, where an intermediate Al_7 core is formed and stabilized (Figure 3a).[8] After adding a 267 nm actinic pump from third-harmonic generation (THG) of FDP, we further investigated the UV-mediated bond cleavage in metal−organic systems such as triphenyl bismuth (Ph_3Bi, Figure 3b) and tungsten hexacarbonyl ($W(CO)_6$, Figure 3c) in organic solvent.[56,57] In the former case, the photoproduct is the crystalline Bi thin film, which exhibits coherent optical phonons in fs transient absorption (fs-TA), while FSRS in the UV region provides high sensitivity for ground-state species due to the peak density of ultrafast pulses versus continuous-wave irradiation.[56] In the latter case, the nascent $W(CO)_5$(solvent) species displays a new visible absorption band as well as different Raman features from $W(CO)_6$ using the ground-state FSRS as a function of UV lamp irradiation time, demonstrating the diversity and significance of photoinduced materials transformation.[57] The power of FSRS in this series of work[8,33,34,56,57] lies in the SRS signal generation by the ps-pump−fs-probe pair. We have also added an actinic pump and used BUMA as the Raman probe to track initial H-bonding dynamics of photoexcited coumarin in solution.[50] Recent work using FSRS to study the dynamics of materials in the solid state (mostly as thin films) has expanded the research scope to molecular heterojunctions, dye-sensitized inorganic colloids for solar cells, and crystalline organic semiconductors for singlet fission.[58−60]

Performing Excited-State FSRS on the Anti-Stokes Side and in the Time−Frequency Domain. Since FSRS gained traction in the field, several variations of basic FSRS themes have appeared in the literature with intriguing comparisons among the observed

DOI: 10.1021/acs.jpclett.8b00373
J. Phys. Chem. Lett. 2018, 9, 3253−3263

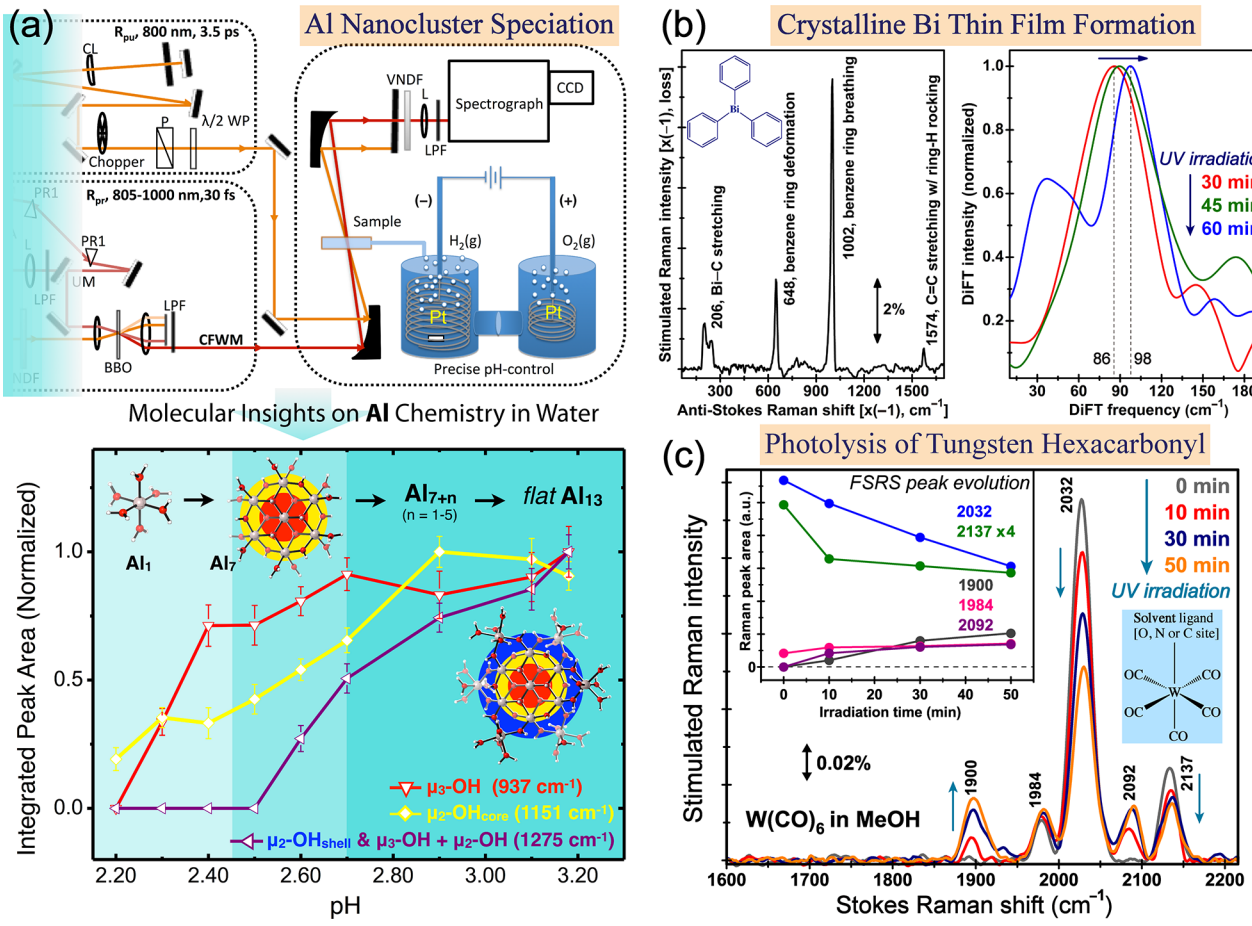

Figure 3. Tracking materials transformation in solution with FSRS. (a) The synergistic use of electrolytic synthesis, BUMA, and FSRS reveals an intermediate Al_7 cluster core en route to the *flat* Al_{13} aqueous cluster as a function of pH. Adapted from ref 8. Copyright 2013, National Academy of Sciences. (b) Ground-state anti-Stokes FSRS of Ph_3Bi in methanol collected with a ~400 nm Raman pump and the UV-BUMA V_{+1} sideband. A blue shift of the retrieved ~90 cm^{-1} phonon mode from the nascent crystalline Bi thin film (i.e., < 100 nm thickness) after 267 nm fs laser irradiation is shown. Reproduced from ref 56. Copyright 2015, AIP Publishing. (c) Time-resolved ground-state FSRS of 20 mM $W(CO)_6$ in methanol after UV lamp irradiation. The evolution of Raman bands tracks consumption of $W(CO)_6$ and accumulation of $W(CO)_5$(solvent) species on the minutes time scale. Adapted from ref 57. Copyright 2016, American Chemical Society.

spectral features.[24,37,38,61] A recent review listed pertinent reports with insightful discussions.[43] In this brief Perspective, we focus on two specific techniques, including ultrafast Raman loss spectroscopy (URLS)[24,25,44,62,63] and time-resolved impulsive stimulated Raman spectroscopy (TR-ISRS)[37,38,47] in comparison with FSRS on the basis of our recent experimental findings.[14,45,53,64] Using a photoacid pyranine, we showed that a combined Stokes and anti-Stokes approach can indeed provide a more complete picture of biphasic vibrational cooling during the excited-state proton transfer (ESPT) reaction.[45] A visible Raman pump that is tunable from ~480−750 nm allows various resonance conditions with the excited-state absorption or stimulated emission bands, which exhibit mode-specific dynamic Raman line shapes from loss, dispersive, to gain particularly for the low-frequency modes on the anti-Stokes FSRS side.[53] The main findings from that work are that both the Raman pump and probe wavelengths contribute to the observed spectral signal line shape and that the ideal resonance enhancement condition for FSRS is not where the Raman pump or probe directly overlaps with the transient electronic peak maximum. Vibrational cooling time constants can also be retrieved from the dynamic FSRS line shape and excited-state Raman mode frequency blue shift during a photoinduced process, more so on the anti-Stokes side than the Stokes side. Notably, the common nature of URLS and anti-Stokes FSRS was established.[25] The benefits of performing these experiments include improved resonance enhancement, better rejection of fluorescence, and higher sensitivity to FC activity and ultrafast vibrational cooling,[39,45,53,62] which could complement the Stokes FSRS in one setting.

Direct observation of an intermolecular H-bond stretching mode between the photoacid pyranine (HPTS) and water molecules from Stokes and anti-Stokes FSRS corroborates the contact ion pair formation and ESPT, facilitated by the anharmonic coupling between Raman-active modes.

On the other research front, to access the low-frequency region, the capable TR-ISRS technique with sub-7 fs pulses was

DOI: 10.1021/acs.jpclett.8b00373
J. Phys. Chem. Lett. 2018, 9, 3253−3263

used to obtain snapshot vibrational spectra.[37,38,47] However, the collection of time-resolved FSRS signal in the frequency domain provides a number of underappreciated benefits. First, efficient data collection in the electronic excited state ensures the integrity of analyzing the transient vibrational intensity, frequency, and bandwidth. If a broad spectral range (e.g., 300−1800 cm^{-1}) at each time delay needs to be covered by scanning two fs pulses, analogous to fs-TA, fine time steps must be used (to Nyquist sample the highest observable frequency) during repeated data scans (to obtain sufficient SNR), therefore requiring long data collection for enough time delay points. Second, the fs−ps−fs pulse sequence ensures balance among photoexcitation, peak density, and a perturbative approach to treat the light−matter interaction using a molecular density matrix and obtain the energy values.[29,42] In contrast, TR-ISRS[37,38] could introduce more higher-order processes, particularly in the FC region. For example, substantial unwanted oscillatory features were observed due to coherent fifth-order processes, which hamper the extraction of intrinsic dynamics of low-frequency modes on the fs time scale.[47] In many cases,[5,14,27,32,46] those early time structural dynamics could hold functional roles in governing the energy, electron, and/or proton transfer pathways. Because the actinic pump simultaneously generates the excited-state population with coherent skeletal motions in FSRS, it provides an in situ platform to decipher functional roles of those low-frequency motions along the photochemical reaction coordinates starting from time zero. For comparison, although the actinic pump can be temporally stretched to avoid inducing coherent motions in TR-ISRS,[47] the delayed arrival of a second fs pump generates coherent motions in an excited-state population that has somewhat relaxed. Therefore, a direct link between observed oscillations and the target anharmonic coupling matrix could be obscured. Third, transient Raman mode dynamics are key observables from FSRS, wherein Raman peaks are heterodyne-detected by the Raman probe; we note that the difference spectral baseline in the electronic excited state could be susceptible to the Raman-pump-induced change to the TA line shape.[14,43,45] Recent experiments have effectively reduced the baseline issue by preresonance enhancement of the excited-state Raman modes, so that small changes to the baseline subtraction lead to negligible differences.[14,45] Because the TR-ISRS approach uses electronic pump−probe signals to track coherent motions that modulate the sample's electronic responses, peak analysis could still be challenging despite the absence of baseline issues because extensive data processing with Fourier transform is required to convert the time-domain oscillations into frequency-domain peaks. In addition, recent discussions on the leading edge of the ps Raman pump effect on the FSRS signal have led to technical modifications using a high-finesse etalon to filter out Raman pump photons that precede the Raman probe.[43] However, several experimental reports have shown that such an effect could be insignificant for the excited-state FSRS mode dynamics of interest.[26,60]

Notably, complications to discern the concurring vibrational coherences require most ISRS experiments to be electronically off-resonant, whereas FSRS can take advantage of resonance Raman enhancement by tuning the ps Raman pump into an electronic transition band. For example, this important strategy has allowed FSRS to produce high-quality Raman spectra of brightly fluorescent molecules.[14,34] Moreover, FSRS requires a tunable ps pump pulse instead of sub-10 fs pulses for the purely time-domain approaches,[9,37,38,48] which are necessary to measure complete maps of excited-state anharmonicities. We stress that these key comparative points are made in this Perspective to substantiate the exploratory and complementary nature of various approaches with the common FSRS theme. At this development stage, stimulating scientific discussions also point out future opportunities to systematically compare the vibrational anharmonicity matrix in a chemically reactive system and reveal key factors that could potentially lead to contrasting results and interpretations, even though the underlying molecular response is generally considered to be identical.[5,37,43,61] The key to observing conformational dynamics of functional relevance is to separate the competing light−matter interaction pathways for reasonable consideration; therefore, clear tracking of the anharmonic vibrational coupling matrix starting from photoexcitation time zero and particularly on the subps time scale can be achieved.

Revealing Functional Relevance of Low-Frequency Motions in Photochemistry. A recent review by Hoffman and Mathies summarized three distinct photoreaction scenarios from weak, moderate, to strong couplings between PESs,[9] predicting that most room-temperature condensed-phase photochemical reactions shorter than ∼10 ps are governed or gated by coherent vibrational dynamics. This point validates the use of FSRS with impulsively excited "modulating/tuning" vibrational coherences and a time-delayed generation of "probing/coupling" vibrational coherences to glean multidimensional chemical reaction coordinates[5,65] while mitigating third-order cascades observed for sidebands in neat solvents.[30,52,66] Particularly, we need to monitor collective skeletal motions (<600 cm^{-1}), which can facilitate photochemistry.[14,67,68] Though less specific or localized than high-frequency modes such as the C−O, C═C or C═N stretches, some low-frequency motions are strongly coupled to certain electronic transitions and other vibrations. Due to impulsive excitation by the fs actinic pump, these low-frequency motions could become coherent in the photoexcited state before damping and dephasing.[5,9,14,32] Direct observation of the anharmonic vibrational coupling between the transient atomic motions is therefore a powerful approach in exposing the multidimensional PES from the electronic ground to excited state(s).

The low-frequency skeletal motions and anharmonic vibrational coupling remain front and center in our quest for a versatile spectroscopic platform to reveal the multidimensional potential energy surface governing photochemistry in action.

Unlike spectral oscillations in transient electronic spectroscopy, the quantum beats observed in FSRS are uniquely poised to dissect coupling between the impulsively excited coherent motions (with the upper-frequency limit dictated by the actinic pump pulse duration) and the vibrational motions being detected (i.e., generated by the ensuing Raman pump−probe pair not limited by the actinic pump duration or initial coherence decay time). The disentanglement of time axes between a sequence of ultrafast laser pulses enables the effective separation between transient vibrational coherences spanning a broad spectral

DOI: 10.1021/acs.jpclett.8b00373
J. Phys. Chem. Lett. 2018, 9, 3253−3263

range.[14,29,32,67] The typical lifetime of impulsively excited vibrational motions is sufficient to exhibit a few periods of characteristic oscillations; therefore, Fourier transform of the observed peak intensity and/or frequency oscillations (i.e., an intensive property for a true fifth-order process)[5,9,65] can map dominant energy relaxation pathways and reaction coordinates in the electronic excited state. This powerful 2D-FSRS approach by tracking the oscillatory behavior of high-frequency modes modulated by low-frequency modes has led to the discovery of a key vibration that powers the classic gene expression marker green fluorescent protein (GFP, see below)[5] and a different low-frequency vibrational mode that facilitates the green emission from a GFP-based calcium biosensor.[32]

Besides such importance, the direct observation of low-frequency modes using FSRS is not a trivial task. We have used a 1:1 (v/v) mixture of CCl_4−ethanol as a solvent standard to calibrate the spectral range of ∼100−1500 cm^{-1} and directly optimize low-frequency mode intensities with the right combination of the Raman pump and probe. The key to implementing low-frequency FSRS lies in the reduction of scattered light into the Raman probe beampath and the "purity" of Raman probe photons in the spectral region close to the Raman pump. Experimental strategies include the following: (1) The sample undergoes microfiltration before FSRS; (2) the incident pulse crossing angle is tuned to increase the intensity and stability of low-frequency modes; (3) several pinholes are placed after the sample to block the scattered light from the Raman pump and actinic pump; (4) with a visible Raman pump, SCWL from a sapphire crystal irradiated by a focused FDP works well because the photon counts are sufficient and the FDP residual is outside of the detection window;[13,14,51] (5) with an ∼800 nm Raman pump, we use the BUMA setup in Figure 2a to generate the Raman probe and collect FSRS signal photons from ∼600 to 830 nm.[8,31,33,34,50]

We first studied FPs and FP-based biosensors because they represent an important class of stimuli-responsive molecules with rich photophysics and photochemistry, also an indispensable toolset for bioimaging and biomedicine. The embedded three-residue chromophore is protected at the center of an 11-stranded β-barrel like a soda can, with the fluorescence quantum yield approaching 0.8 for the wild-type (wt)GFP.[6,69,70] Earlier work by Fang et al.[5] reported a phenolic ring out-of-plane wagging motion at ∼120 cm^{-1}, which modulates the distance between the wtGFP chromophore phenolic hydroxyl and the adjacent conserved water molecule. Interestingly, for a GFP-calmodulin (CaM) chimeric Ca^{2+} biosensor, GEM-GECO1,[71] we captured vibrational intensity quantum beats (Figure 4c) and unveiled a ∼170 cm^{-1} phenol ring in-plane rocking motion (i.e., different from wtGFP) that modulates the distance between the chromophore phenolic hydroxyl group and a nearby serine residue (Figure 4d). These distances essentially correspond to the proton donor and acceptor interaction strength along the H-bonding chain and hence affect the ESPT rate.[6,13,72] Furthermore, labile water molecules act as a bridge due to solvent exposure via the β-barrel opening.[32] Such spectral oscillations in frequency and intensity arise from the third-order anharmonic coupling terms between vibrational modes in the electronic excited state, which are uniquely tracked by FSRS.[5,32,46] The Raman mode assignment of the chromophore is aided by density functional theory (DFT) and time-dependent (TD)-DFT calculations[73] with local structural constraints either from crystal structures[5,70] or from the equilibrated structures in molecular dynamics (MD) simulations.[32,72]

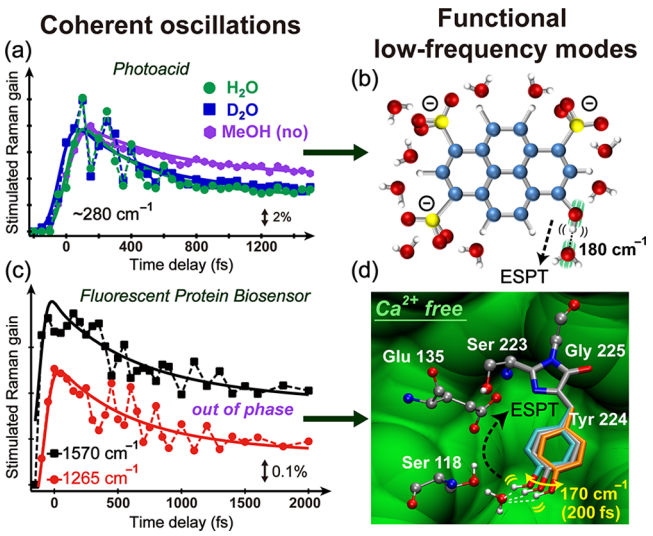

Figure 4. Low-frequency motions can be functional for photochemistry. (a) Raman intensity oscillations of a 280 cm^{-1} ring deformation mode of the photoacid HPTS on the subps time scale are prominent in an aqueous solution that supports ESPT but insignificant in methanol that inhibits ESPT. Adapted from ref 14. Copyright 2016, Royal Society of Chemistry. (b) The retrieved ∼180 cm^{-1} modulation mode corresponds to an intermolecular H-bonding motion between the HPTS hydroxyl end and a solvent molecule. (c) Raman intensity oscillations of the 1265 (red) and 1570 (black) cm^{-1} modes of the Ca^{2+}-free GEM-GECO1 biosensor reveal quantum beating with a period of ∼200 fs. (d) Depiction of the ∼170 cm^{-1} phenolic ring rocking mode (yellow) that gates the ESPT reaction inside of the biosensor. Dashed arrows in (b) and (d) indicate the ESPT directions. Adapted from ref 32. Copyright 2014, National Academy of Sciences.

The aforementioned FP chromophore can be viewed as a photoacid inside of a protein matrix. To provide deeper insights into molecular photoacidity acting as the driving force for ESPT, a comparative study on model photoacids in solution is warranted. New evidence supporting the functionality of key low-frequency modes has emerged from our systematic investigation of the photoacid HPTS in solution,[14,27,28,45] complementing the time-resolved IR reports focusing on high-frequency modes such as the C═O or O−H stretching.[11,74] The formation of a contact ion pair was proposed on the basis of time-resolved electronic spectra[75] to understand the origin of two time constants of ∼3 and 90 ps for ESPT reaction. Our recent FSRS data have provided the crucial structural resolution at the chemical bond level to evaluate initial processes with spectral oscillations, low-frequency modes, and ultrafast vibrational cooling, which elucidate primary molecular events powering ESPT in water. Notably for the photoexcited HPTS undergoing ESPT to convert protonated form PA* to the deprotonated form PB* before fluorescence, (1) intensity quantum beating of a 280 cm^{-1} ring out-of-plane deformation mode is observed in solvents that support ESPT, such as H_2O, D_2O, and $H_2{}^{18}O$, but not in methanol, which inhibits ESPT (Figure 4a),[14] (2) the 180 cm^{-1} intermolecular H-bond stretching mode (Figure 4b) shows biphasic decay time constants of ∼500 fs and 45 ps due to ultrafast vibrational cooling,[14,45] (3) a typical ∼1 ps dwell for PB* rise corroborates the existence of contact ion pairs because without them we would see the concomitant PA* decay and PB* rise,[14,27,28] and (4) the anti-Stokes FSRS data reveal that the 420 cm^{-1} ring in-plane deformation mode in S_1 exhibits a biphasic frequency blue shift with time constants of ∼2.2 and 45 ps in pH = 4.5 water and 9.4 and 56 ps in

DOI: 10.1021/acs.jpclett.8b00373
J. Phys. Chem. Lett. 2018, 9, 3253−3263

methanol, respectively.[45] Notably, this previously hidden time constant of 45 ps in water is uncovered from the 180 cm^{-1} mode intensity dynamics in Stokes FSRS and the 420 cm^{-1} mode blue shift in anti-Stokes FSRS, associated with vibrational cooling from the first solvation shell to bulk solvent.

> Systematic chemical modification methods include organic synthesis, site-specific mutagenesis with canonical amino acids, and genetic code expansion with noncanonical amino acids in physiological environments.

Comparison between these proton-transfer and vibrational cooling time constants leads to a unifying description of incipient structural dynamics of ESPT, which substantiates the contact ion pair as an integral part of proton motion. The reasons are as follows: First, on the subps time scale, the impulsively excited H-bond stretching mode modulates the chromophore ring deformation mode via anharmonic coupling. Second, on the few ps time scale, initial vibrational cooling and energy redistribution help form the contact ion pair, while the H-bond stretching mode acts as a conduit/bridge for energy/proton transfer within the first solvation shell. Third, on the tens of ps time scale, while ESPT proceeds via separation of the contact ion pair and further solvation of the deprotonated chromophore and proton, the low-frequency modes sense thermal cooling from first solvation shell to bulk solvent, which no longer track ESPT.[14,45] This level of knowledge arises from the observed low-frequency mode dynamics in different environments on ultrafast time scales starting from photoexcitation time zero and the comparative analysis aided by high-frequency vibrational dynamics, tunable fs-TA results, and quantum calculations.[5,14,68]

From Mechanistic Understanding, Chemical Modification, to Rational Design. Upon first glance, FSRS characterization of FPs and biosensors in action may seem "specialized" because they entail a large stack of evolving spectra on ultrafast time scales. However, these transient Raman spectra offer a rare window to peek into the dynamic world of a chromophore when photons strike, revealing fluorescence mechanisms that power various applications in materials, energy, and life sciences. Notably, current development of molecular machines mainly arises from trial and error, which works but lacks efficiency or oversight. It will be imperative and beneficial to translate the vibrational signatures, atomic motions, and hidden reaction coordinates uncovered by FSRS into targeted design principles for next-generation molecular machines.

The first experimental strategy is chemical modification and systematic evaluation of the resultant functionality change. The chromophores that we have studied typically contain a phenolic hydroxyl; therefore, the ring provides some electron-withdrawing property that leads to charge transfer upon electronic excitation. The logical next step involves substituting functional groups around the aromatic scaffold. Figure 5a presents our recent efforts in studying GFP model chromophore *p*-hydroxybenzylidene-imidazolidinone (*p*-HOBDI), in comparison to its conformationally locked derivatives *p*-HOBDI-BF_2 and *p*-HO-3,5-diF-BDI:BF_2 (abbreviated as diF) via organic synthesis, which "regain" fluorescence.[76] The time-resolved Stokes FSRS intensity

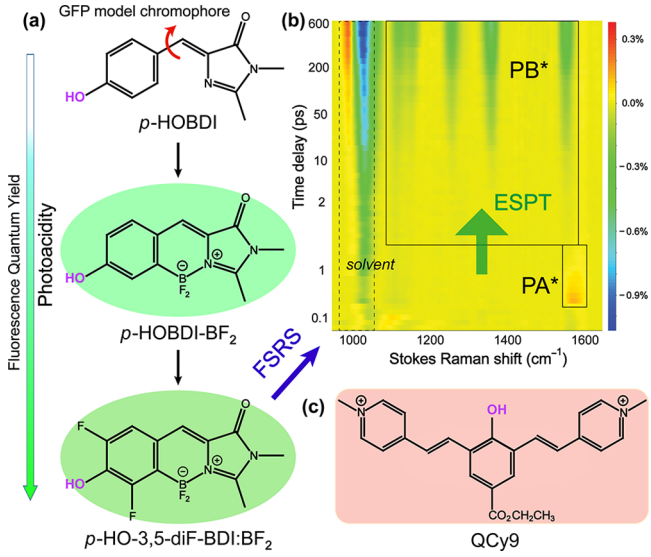

Figure 5. Photoacidity is dissected by FSRS to correlate the chemical modification and targeted molecular functionality. (a) Enhancement of ESPT capability and fluorescence quantum yield by adding functional groups to the GFP model chromophore. Conformational locking by a BF_2 group inhibits ring twisting and enables strong fluorescence after ESPT, while the addition of electronegative fluorines further increases photoacidity. (b) Time-resolved FSRS contour plot of diF in methanol after 400 nm photoexcitation. On the subps time scale, PA* dissociation occurs, as shown by the ~1580 cm^{-1} mode. On the ps time scale, PB* accumulation is assisted by diffusion. Solid boxes highlight prominent photoacid transient species, while the dashed box indicates solvent features (mainly the methanol C−O stretching motion with dispersive line shapes in the excited-state difference spectrum). (c) The strongest synthetic photoacid to date, QCy9, is a model system for ESPT beyond the solvent-control limit, albeit with low fluorescence.

contour plot in Figure 5b with a 510 nm Raman pump shows desirable resonance enhancement for diF in solution, achieved by strategically tuning the Raman pump in between stimulated emission bands of the protonated (PA*) and deprotonated (PB*) chromophores.[64] The dwell between PA* decay and PB* rise indicates an intermediate charge-separated state that likely involves initial proton dissociation on the ~600 fs time scale, which is corroborated by the fs-TA results. The unusual FSRS signal sign reversal in Figure 5b is attributed to different resonance conditions for transient PA* and PB* species with a fixed Raman pump,[45] in particular, the relative position of the Raman probe on the anti-Stokes or Stokes side with reference to the stimulated emission band maximum (i.e., the negative peak position).[45,53] The mode-dependent vibrational dynamics in the electronic excited state reveal the key atomic motions facilitating the ESPT reaction onset, particularly the 1580 cm^{-1} phenolic ring motion (see the PA* mode in Figure 5b). In comparison, the superphotoacidity of a synthetic phenol cyanine dye QCy9 (Figure 5c) provides a further expanded aromatic framework with more structural flexibilities. This series of investigations of modifiable fluorophores therefore allows us to examine the ultrafast competition between ESPT and conjugated ring twisting motions in close correlation with the fluorescence outcome.[51,77]

The second strategy targeting FPs is to chemically modify the protein chromophore via genetic code expansion methods.[78] In a proof-of-principle investigation, we designed a single-site Pro377Arg mutant that effectively changes the GEM-GECO1

DOI: 10.1021/acs.jpclett.8b00373
J. Phys. Chem. Lett. 2018, 9, 3253−3263

biosensor[32] from green-blue emission ratiometric to green excitation ratiometric while unveiling the hidden protein chromophore conformational inhomogeneity.[46] We have systematically compared the FSRS data from noncanonical incorporations of various halogens and amino and nitro groups to the phenolic ring of the superfolder (sf)GFP chromophore in order to reveal key structural motions and functional motifs around the proton dissociation site governing characteristic FP emission properties (Figure 6). A detailed study of the effect of functional group

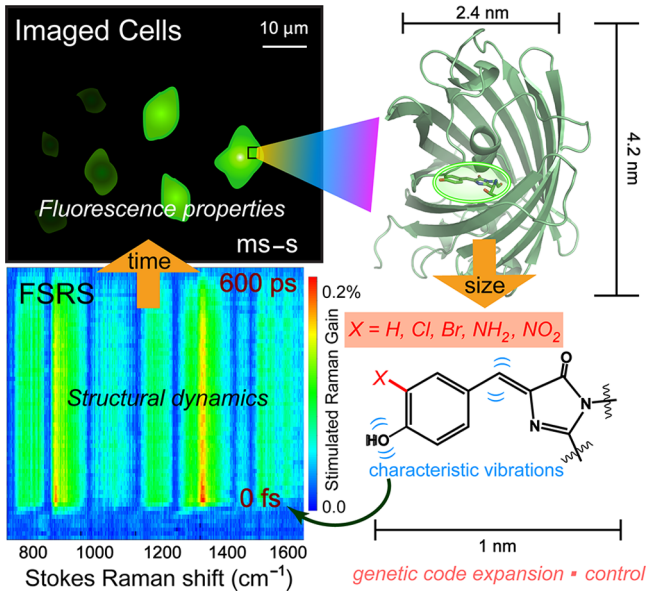

Figure 6. Rational design of protein functionality with genetic code expansion and FSRS. (Clockwise from upper left to bottom left) Cells are imaged in vivo with the genetically encoded FPs, which under a sequence of wavelength-tunable light irradiation, can be studied in vitro on atomic levels (orange downward arrow) and molecular time scales. The GFP chromophore is highlighted by the green ellipse, and X (red) in the chromophore chemical structure can be precisely tuned from hydrogen, halogens, amino, to nitro groups. The Stokes FSRS contour plot delineates transient Raman mode decay of the photoexcited (λ_{ex} = 480 nm, R_{pu} = 550 nm) 3Br-sfGFP deprotonated chromophore on the ps time scale prior to fluorescence. On much longer time scales (orange upward arrow), macroscopic emission properties can be improved (e.g., brighter, red-shifted) on the basis of microscopic insights, completing the bottom-up design loop.

substitutions from strongly electron-donating (e.g., NH_2) to -withdrawing (e.g, Cl, Br, NO_2) on the chromophore aromatic rings, from a solution environment (Figure 5) to the protein interior (Figure 6), is ongoing in our laboratory and will yield important insights into the structure–energy–function relationships of these fluorescent molecules.

Using a similar control strategy, McCamant, Scholes, and co-workers implemented FSRS to study four related cryptophyte light-harvesting proteins grown and isolated from algae, which helps to pinpoint the origin of spectral oscillations in TA data.[79] The carefully designed experiment made use of structurally similar phycobiliproteins with different electronic and vibrational levels, hence providing a platform to discern the correlation between the excitation frequency and response frequency, distinguish the ground- and excited-state coherences, as well as differentiate electronic coupling from vibronic coupling. Tuning the central frequency of the pump pulse in TA was mentioned for their future experiments, which could be enhanced by an excited-state FSRS study with a tunable Raman pump–probe pair (see above) to directly expose the photoinduced transient vibrational modes of the related proteins.[32,51,80]

Summary and Perspectives on Future Directions. Following ~15 years of seminal work in the experimental and theoretical FSRS fields, an exciting research avenue has emerged in dissecting photochemistry in the condensed phase frame by frame.[9,43,67] The practicality and versatility of tunable FSRS (evinced by the first commercially available turn-key FSRS spectrometer by Newport Corp. in 2017) originate from utilization of optical laser pulses in exposing atomic motions, which provide a unique window to track coupled electronic and nuclear motions as they occur on molecular time scales starting from a precise time zero set by the actinic pump. Using ultrafast Raman spectroscopic methodology, the structure–function relationships of a wide array of functional molecules from metal–organic complexes, semiconductor thin films, DNA bases, photoacids, to FP-based calcium biosensors has been revealed (see Figure 1 for example). By tracking coherent low-frequency motions from the time zero of photoexcitation and resolving the anharmonically coupled vibrational dynamics, their functional roles can be established with vivid details that benefit from the technical innovations of the FSRS technology, as discussed above.

Furthermore, tunable FSRS has recently yielded valuable insights into the conformational heterogeneity of protein chromophores (typically hidden beneath a broad spectral line shape) that exhibit a range of geometric constraints, H-bonding configurations, and proton-transfer rates,[46,51,72] reminiscent of recent findings from cryo-EM that suggest a continuous variation in conformational space and free-energy landscapes for biomolecules in solution.[81] Interestingly, McCamant and co-workers used tunable FSRS with a UV pump to study a common nucleic acid derivative dGMP and uncovered a structurally inhomogeneous population in a largely flat PES before its relaxation back to the ground state via a conical intersection.[82] Ultrafast Raman spectroscopy also revealed local structural disorder, heterogeneity, and effects on dynamics such as exciton trapping in photoexcited conjugated materials.[41] This line of inquiry substantiates the importance of adopting a combinatorial approach with TA and tunable FSRS, aided by quantum mechanical and MD calculations, in revealing the structural heterogeneity and characteristic dynamics with specific molecular species and populations.

Looking forward, several challenges remain for FSRS experiments that mainly concern the sample states, standardized data processing, and better correlation between structure and energy. Improved optical setup and scattering minimization methods are required for data collection from the solid-state samples, ideally in ambient conditions with less stringent requirements for thickness or crystallinity. A reflection instead of transmission configuration may provide an appealing alternative to record the FSRS signal being collinear and heterodyned by the reflected Raman probe beam. Technical advances in laser technology could provide bluer pulses in the far-UV and redder pulses in the near-IR region to further expand the spectral window with desired resonance enhancement in the ground or excited state. Such optimized resonance conditions have the potential to minimize the baseline issues that currently affect FSRS especially when the excited states are involved.[14,35,64,83] Shorter pulses and optimization of the Raman pump–probe duration, power, wavelength, and shape are necessary to achieve the best signal-to-noise ratio in the time-resolved excited-state FSRS and 2D FSRS. Exciting advances have hitherto been

DOI: 10.1021/acs.jpclett.8b00373
J. Phys. Chem. Lett. 2018, 9, 3253–3263

discussed[34,38,43,44,50,60,64,83] with a common theme in addressing deficiencies or complexities of certain aspects of FSRS for it to further evolve into a robust and user-friendly technique.

With hindsight and looking forward, FSRS has a bright future as an integral part of a ultrafast spectroscopic toolset in elucidating structural dynamics of functional molecular machines powering energy and biological systems.

We note that the true power of ultrafast time−frequency Raman spectroscopy in the electronic excited state lies not only in the depth of information gained from one particular system but also in the breadth of systems that can be studied. The complexity of a macromolecule such as a protein biosensor may prevent us from revealing every molecular aspect affecting its function, but it is highly feasible to change a specific part of the molecule and monitor its consequence in solution and protein environments. Systematic comparison between carefully designed control experiments has been proven effective toward a true mechanistic understanding. As a result, the multidimensional reactive PES can be dissected by tunable FSRS, one coordinate at a time.

AUTHOR INFORMATION

Corresponding Author

*E-mail: Chong.Fang@oregonstate.edu. Phone: (541) 737-6704.

ORCID

Chong Fang: 0000-0002-8879-1825
Longteng Tang: 0000-0001-9316-188X
Breland G. Oscar: 0000-0001-7919-5442
Cheng Chen: 0000-0003-0561-5226

Notes

The authors declare no competing financial interest.

Biographies

Chong Fang graduated from the University of Science and Technology of China (USTC) with a B.S. degree in Chemistry and Applied Computer Science (dual degree) in 2001. He obtained a Ph.D. in Physical Chemistry from the University of Pennsylvania in 2006 under the direction of Robin M. Hochstrasser. After postdoctoral research at the University of California, Berkeley with Richard A. Mathies, Dr. Fang joined the faculty of Department of Chemistry at Oregon State University in 2010. He has been Associate Professor since 2016, and his research focuses on developing and implementing ultrafast optical and vibrational spectroscopy to elucidate structural dynamics governing molecular functionality in materials and biological sciences.

Longteng Tang received his B.S. degree in Chemistry from Renmin University of China in 2010 and obtained his Ph.D. degree (Physical Chemistry) at Oregon State University in 2017. His research has focused on the fluorescence mechanisms of calcium biosensors and photoacids.

Breland G. Oscar received her B.S. degree in Chemistry from Sewanee: The University of the South in 2011 and obtained her Ph.D. degree (Physical Chemistry) at Oregon State University in 2017. Her research has focused on structural dynamics of calcium biosensors and fluorescent proteins with noncanonical amino acids.

Cheng Chen received his B.S. degree in Chemistry from the University of Science and Technology of China (USTC) in 2013 and is currently a Ph.D. candidate at Oregon State University. His research has focused on ultrafast dynamics of the synthetic superphotoacids and redder chromophores in solution.

ACKNOWLEDGMENTS

This work was supported by the NSF CAREER Grant (CHE-1455353), OSU Faculty Research Start-Up Grant (2010−2016), OSU General Research Fund and Research Equipment Reserve Fund (Spring 2014), and Oregon Medical Research Foundation New Investigator Grant (2016−2017) to C.F. The authors thank their collaborators Yongxin Zhao, Robert E. Campbell, Wei Wang, Sumit Saha, Douglas A. Keszler, Ryan A. Mehl, Kyril M. Solntsev, Mikhail S. Baranov, and Dan Huppert, together with current and former group members, particularly Weimin Liu, Liangdong Zhu, Yanli Wang, Liang Wang, and Fangyuan Han.

REFERENCES

(1) Wang, Q.; Schoenlein, R. W.; Peteanu, L. A.; Mathies, R. A.; Shank, C. V. Vibrationally Coherent Photochemistry in the Femtosecond Primary Event of Vision. *Science* **1994**, *266*, 422−424.

(2) Zewail, A. H. *Femtochemistry: Ultrafast Dynamics of the Chemical Bond*; World Scientific: Singapore, 1994.

(3) Kukura, P.; McCamant, D. W.; Yoon, S.; Wandschneider, D. B.; Mathies, R. A. Structural Observation of the Primary Isomerization in Vision with Femtosecond-Stimulated Raman. *Science* **2005**, *310*, 1006−1009.

(4) Engel, G. S.; Calhoun, T. R.; Read, E. L.; Ahn, T.-K.; Mancal, T.; Cheng, Y.-C.; Blankenship, R. E.; Fleming, G. R. Evidence for Wavelike Energy Transfer through Quantum Coherence in Photosynthetic Systems. *Nature* **2007**, *446*, 782−786.

(5) Fang, C.; Frontiera, R. R.; Tran, R.; Mathies, R. A. Mapping GFP Structure Evolution during Proton Transfer with Femtosecond Raman Spectroscopy. *Nature* **2009**, *462*, 200−204.

(6) Meech, S. R. Excited State Reactions in Fluorescent Proteins. *Chem. Soc. Rev.* **2009**, *38*, 2922−2934.

(7) Collini, E.; Wong, C. Y.; Wilk, K. E.; Curmi, P. M. G.; Brumer, P.; Scholes, G. D. Coherently Wired Light-Harvesting in Photosynthetic Marine Algae at Ambient Temperature. *Nature* **2010**, *463*, 644−647.

(8) Wang, W.; Liu, W.; Chang, I.-Y.; Wills, L. A.; Zakharov, L. N.; Boettcher, S. W.; Cheong, P. H.-Y.; Fang, C.; Keszler, D. A. Electrolytic Synthesis of Aqueous Aluminum Nanoclusters and *in situ* Characterization by Femtosecond Raman Spectroscopy and Computations. *Proc. Natl. Acad. Sci. U. S. A.* **2013**, *110*, 18397−18401.

(9) Hoffman, D. P.; Mathies, R. A. Femtosecond Stimulated Raman Exposes the Role of Vibrational Coherence in Condensed-Phase Photoreactivity. *Acc. Chem. Res.* **2016**, *49*, 616−625.

(10) Miller, R. J. D. Femtosecond Crystallography with Ultrabright Electrons and X-Rays: Capturing Chemistry in Action. *Science* **2014**, *343*, 1108−1116.

(11) Rini, M.; Magnes, B.-Z.; Pines, E.; Nibbering, E. T. J. Real-Time Observation of Bimodal Proton Transfer in Acid-Base Pairs in Water. *Science* **2003**, *301*, 349−352.

(12) Westlake, B. C.; Brennaman, M. K.; Concepcion, J. J.; Paul, J. J.; Bettis, S. E.; Hampton, S. D.; Miller, S. A.; Lebedeva, N. V.; Forbes, M. D. E.; Moran, A. M.; et al. Concerted Electron-Proton Transfer in the Optical Excitation of Hydrogen-Bonded Dyes. *Proc. Natl. Acad. Sci. U. S. A.* **2011**, *108*, 8554−8558.

(13) Tang, L.; Liu, W.; Wang, Y.; Zhao, Y.; Oscar, B. G.; Campbell, R. E.; Fang, C. Unraveling Ultrafast Photoinduced Proton Transfer Dynamics in a Fluorescent Protein Biosensor for Ca^{2+} Imaging. *Chem. - Eur. J.* **2015**, *21*, 6481−6490.

(14) Liu, W.; Wang, Y.; Tang, L.; Oscar, B. G.; Zhu, L.; Fang, C. Panoramic Portrait of Primary Molecular Events Preceding Excited State Proton Transfer in Water. *Chem. Sci.* **2016**, *7*, 5484−5494.

DOI: 10.1021/acs.jpclett.8b00373
J. Phys. Chem. Lett. 2018, 9, 3253−3263

(15) Freudiger, C. W.; Min, W.; Saar, B. G.; Lu, S.; Holtom, G. R.; He, C.; Tsai, J. C.; Kang, J. X.; Xie, X. S. Label-Free Biomedical Imaging with High Sensitivity by Stimulated Raman Scattering Microscopy. *Science* **2008**, *322*, 1857−1861.
(16) Saar, B. G.; Freudiger, C. W.; Reichman, J.; Stanley, C. M.; Holtom, G. R.; Xie, X. S. Video-Rate Molecular Imaging In Vivo with Stimulated Raman Scattering. *Science* **2010**, *330*, 1368−1370.
(17) Yoshizawa, M.; Kurosawa, M. Femtosecond Time-Resolved Raman Spectroscopy Using Stimulated Raman Scattering. *Phys. Rev. A: At., Mol., Opt. Phys.* **1999**, *61*, 013808.
(18) McCamant, D. W.; Kukura, P.; Yoon, S.; Mathies, R. A. Femtosecond Broadband Stimulated Raman Spectroscopy: Apparatus and Methods. *Rev. Sci. Instrum.* **2004**, *75*, 4971−4980.
(19) Lee, S.-Y.; Zhang, D.; McCamant, D. W.; Kukura, P.; Mathies, R. A. Theory of Femtosecond Stimulated Raman Spectroscopy. *J. Chem. Phys.* **2004**, *121*, 3632−3642.
(20) Laimgruber, S.; Schachenmayr, H.; Schmidt, B.; Zinth, W.; Gilch, P. A Femtosecond Stimulated Raman Spectrograph for the Near Ultraviolet. *Appl. Phys. B: Lasers Opt.* **2006**, *85*, 557−564.
(21) Frontiera, R. R.; Shim, S.; Mathies, R. A. Origin of Negative and Dispersive Features in Anti-Stokes and Resonance Femtosecond Stimulated Raman Spectroscopy. *J. Chem. Phys.* **2008**, *129*, 064507.
(22) Takeuchi, S.; Ruhman, S.; Tsuneda, T.; Chiba, M.; Taketsugu, T.; Tahara, T. Spectroscopic Tracking of Structural Evolution in Ultrafast Stilbene Photoisomerization. *Science* **2008**, *322*, 1073−1077.
(23) Dasgupta, J.; Frontiera, R. R.; Taylor, K. C.; Lagarias, J. C.; Mathies, R. A. Ultrafast Excited-State Isomerization in Phytochrome Revealed by Femtosecond Stimulated Raman Spectroscopy. *Proc. Natl. Acad. Sci. U. S. A.* **2009**, *106*, 1784−1789.
(24) Umapathy, S.; Lakshmanna, A.; Mallick, B. Ultrafast Raman Loss Spectroscopy. *J. Raman Spectrosc.* **2009**, *40*, 235−237.
(25) Qiu, X.; Li, X.; Niu, K.; Lee, S.-Y. Inverse Raman Bands in Ultrafast Raman Loss Spectroscopy. *J. Chem. Phys.* **2011**, *135*, 164502.
(26) Weigel, A.; Dobryakov, A.; Klaumünzer, B.; Sajadi, M.; Saalfrank, P.; Ernsting, N. P. Femtosecond Stimulated Raman Spectroscopy of Flavin after Optical Excitation. *J. Phys. Chem. B* **2011**, *115*, 3656−3680.
(27) Liu, W.; Han, F.; Smith, C.; Fang, C. Ultrafast Conformational Dynamics of Pyranine during Excited State Proton Transfer in Aqueous Solution Revealed by Femtosecond Stimulated Raman Spectroscopy. *J. Phys. Chem. B* **2012**, *116*, 10535−10550.
(28) Han, F.; Liu, W.; Fang, C. Excited-State Proton Transfer of Photoexcited Pyranine in Water Observed by Femtosecond Stimulated Raman Spectroscopy. *Chem. Phys.* **2013**, *422*, 204−219.
(29) Dorfman, K. E.; Fingerhut, B. P.; Mukamel, S. Time-Resolved Broadband Raman Spectroscopies: A Unified Six-Wave-Mixing Representation. *J. Chem. Phys.* **2013**, *139*, 124113.
(30) Dunlap, B.; Wilson, K. C.; McCamant, D. W. Phase-Matching and Dilution Effects in Two-Dimensional Femtosecond Stimulated Raman Spectroscopy. *J. Phys. Chem. A* **2013**, *117*, 6205−6216.
(31) Zhu, L.; Liu, W.; Fang, C. Tunable Sideband Laser from Cascaded Four-Wave Mixing in Thin Glass for Ultra-Broadband Femtosecond Stimulated Raman Spectroscopy. *Appl. Phys. Lett.* **2013**, *103*, 061110.
(32) Oscar, B. G.; Liu, W.; Zhao, Y.; Tang, L.; Wang, Y.; Campbell, R. E.; Fang, C. Excited-State Structural Dynamics of a Dual-Emission Calmodulin-Green Fluorescent Protein Sensor for Calcium Ion Imaging. *Proc. Natl. Acad. Sci. U. S. A.* **2014**, *111*, 10191−10196.
(33) Zhu, L.; Liu, W.; Fang, C. A Versatile Femtosecond Stimulated Raman Spectroscopy Setup with Tunable Pulses in the Visible to Near Infrared. *Appl. Phys. Lett.* **2014**, *105*, 041106.
(34) Zhu, L.; Liu, W.; Wang, Y.; Fang, C. Sum-Frequency-Generation-Based Laser Sidebands for Tunable Femtosecond Raman Spectroscopy in the Ultraviolet. *Appl. Sci.* **2015**, *5*, 48−61.
(35) Quick, M.; Dobryakov, A. L.; Kovalenko, S. A.; Ernsting, N. P. Resonance Femtosecond-Stimulated Raman Spectroscopy without Actinic Excitation Showing Low-Frequency Vibrational Activity in the S_2 State of All-Trans β-Carotene. *J. Phys. Chem. Lett.* **2015**, *6*, 1216−1220.
(36) Molesky, B. P.; Guo, Z.; Moran, A. M. Femtosecond Stimulated Raman Spectroscopy by Six-Wave Mixing. *J. Chem. Phys.* **2015**, *142*, 212405.
(37) Liebel, M.; Schnedermann, C.; Wende, T.; Kukura, P. Principles and Applications of Broadband Impulsive Vibrational Spectroscopy. *J. Phys. Chem. A* **2015**, *119*, 9506−9517.
(38) Kuramochi, H.; Takeuchi, S.; Tahara, T. Femtosecond Time-Resolved Impulsive Stimulated Raman Spectroscopy using Sub-7-fs Pulses: Apparatus and Applications. *Rev. Sci. Instrum.* **2016**, *87*, 043107.
(39) Batignani, G.; Pontecorvo, E.; Giovannetti, G.; Ferrante, C.; Fumero, G.; Scopigno, T. Electronic Resonances in Broadband Stimulated Raman Spectroscopy. *Sci. Rep.* **2016**, *6*, 18445.
(40) Buchanan, L. E.; Gruenke, N. L.; McAnally, M. O.; Negru, B.; Mayhew, H. E.; Apkarian, V. A.; Schatz, G. C.; Van Duyne, R. P. Surface-Enhanced Femtosecond Stimulated Raman Spectroscopy at 1 MHz Repetition Rates. *J. Phys. Chem. Lett.* **2016**, *7*, 4629−4634.
(41) Bragg, A. E.; Yu, W.; Zhou, J.; Magnanelli, T. Ultrafast Raman Spectroscopy as a Probe of Local Structure and Dynamics in Photoexcited Conjugated Materials. *J. Phys. Chem. Lett.* **2016**, *7*, 3990−4000.
(42) Wu, Y.-C.; Zhao, B.; Lee, S.-Y. Time-Dependent Wave Packet Averaged Vibrational Frequencies from Femtosecond Stimulated Raman Spectra. *J. Chem. Phys.* **2016**, *144*, 054104.
(43) Dietze, D. R.; Mathies, R. A. Femtosecond Stimulated Raman Spectroscopy. *ChemPhysChem* **2016**, *17*, 1224−1251.
(44) Roy, K.; Kayal, S.; Ariese, F.; Beeby, A.; Umapathy, S. Mode Specific Excited State Dynamics Study of Bis(phenylethynyl)benzene from Ultrafast Raman Loss Spectroscopy. *J. Chem. Phys.* **2017**, *146*, 064303.
(45) Liu, W.; Tang, L.; Oscar, B. G.; Wang, Y.; Chen, C.; Fang, C. Tracking Ultrafast Vibrational Cooling During Excited State Proton Transfer Reaction with Anti-Stokes and Stokes Femtosecond Stimulated Raman Spectroscopy. *J. Phys. Chem. Lett.* **2017**, *8*, 997−1003.
(46) Tachibana, S. R.; Tang, L.; Wang, Y.; Zhu, L.; Liu, W.; Fang, C. Tuning Calcium Biosensors with a Single-Site Mutation: Structural Dynamics Insights from Femtosecond Raman Spectroscopy. *Phys. Chem. Chem. Phys.* **2017**, *19*, 7138−7146.
(47) Kuramochi, H.; Takeuchi, S.; Yonezawa, K.; Kamikubo, H.; Kataoka, M.; Tahara, T. Probing the Early Stages of Photoreception in Photoactive Yellow Protein with Ultrafast Time-Domain Raman Spectroscopy. *Nat. Chem.* **2017**, *9*, 660−666.
(48) Batignani, G.; Fumero, G.; Mukamel, S.; Scopigno, T. Energy Flow between Spectral Components in 2D Broadband Stimulated Raman Spectroscopy. *Phys. Chem. Chem. Phys.* **2015**, *17*, 10454−10461.
(49) Kowalewski, M.; Mukamel, S. Stimulated Raman Signals at Conical Intersections: *Ab initio* Surface Hopping Simulation Protocol with Direct Propagation of the Nuclear Wave Function. *J. Chem. Phys.* **2015**, *143*, 044117.
(50) Han, F.; Liu, W.; Zhu, L.; Wang, Y.; Fang, C. Initial Hydrogen-Bonding Dynamics of Photoexcited Coumarin in Solution with Femtosecond Stimulated Raman Spectroscopy. *J. Mater. Chem. C* **2016**, *4*, 2954−2963.
(51) Tang, L.; Liu, W.; Wang, Y.; Zhu, L.; Han, F.; Fang, C. Ultrafast Structural Evolution and Chromophore Inhomogeneity inside a Green-Fluorescent-Protein-Based Ca^{2+} Biosensor. *J. Phys. Chem. Lett.* **2016**, *7*, 1225−1230.
(52) Zhao, B.; Niu, K.; Li, X.; Lee, S.-Y. Simple Aspects of Femtosecond Stimulated Raman Spectroscopy. *Sci. China: Chem.* **2011**, *54*, 1989−2008.
(53) Oscar, B. G.; Chen, C.; Liu, W.; Zhu, L.; Fang, C. Dynamic Raman Lineshapes on an Evolving Excited State Landscape: Insights from Tunable Femtosecond Stimulated Raman Spectroscopy. *J. Phys. Chem. A* **2017**, *121*, 5428−5441.
(54) Liu, W.; Zhu, L.; Wang, L.; Fang, C. Cascaded Four-Wave Mixing for Broadband Tunable Laser Sideband Generation. *Opt. Lett.* **2013**, *38*, 1772−1774.

DOI: 10.1021/acs.jpclett.8b00373
J. Phys. Chem. Lett. 2018, 9, 3253−3263

(55) Zhu, L.; Liu, W.; Wang, L.; Fang, C. Parametric Amplification-Assisted Cascaded Four-Wave Mixing for Ultrabroad Laser Sideband Generation in a Thin Transparent Medium. *Laser Phys. Lett.* **2014**, *11*, 075301.
(56) Zhu, L.; Saha, S.; Liu, W.; Wang, Y.; Keszler, D. A.; Fang, C. Simultaneous Solution-Based Generation and Characterization of Crystalline Bismuth Thin Film by Femtosecond Laser Spectroscopy. *Appl. Phys. Lett.* **2015**, *107*, 061901.
(57) Zhu, L.; Saha, S.; Wang, Y.; Keszler, D. A.; Fang, C. Monitoring Photochemical Reaction Pathways of Tungsten Hexacarbonyl in Solution from Femtoseconds to Minutes. *J. Phys. Chem. B* **2016**, *120*, 13161−13168.
(58) Frontiera, R. R.; Dasgupta, J.; Mathies, R. A. Probing Interfacial Electron Transfer in Coumarin 343 Sensitized TiO2 Nanoparticles with Femtosecond Stimulated Raman. *J. Am. Chem. Soc.* **2009**, *131*, 15630−15632.
(59) Provencher, F.; Bérubé, N.; Parker, A. W.; Greetham, G. M.; Towrie, M.; Hellmann, C.; Côté, M.; Stingelin, N.; Silva, C.; Hayes, S. C. Direct Observation of Ultrafast Long-Range Charge Separation at Polymer−Fullerene Heterojunctions. *Nat. Commun.* **2014**, *5*, 4288.
(60) Hart, S. M.; Silva, W. R.; Frontiera, R. R. Femtosecond Stimulated Raman Evidence for Charge-Transfer Character in Pentacene Singlet Fission. *Chem. Sci.* **2018**, *9*, 1242−1250.
(61) Fujisawa, T.; Kuramochi, H.; Hosoi, H.; Takeuchi, S.; Tahara, T. Role of Coherent Low-Frequency Motion in Excited-State Proton Transfer of Green Fluorescent Protein Studied by Time-Resolved Impulsive Stimulated Raman Spectroscopy. *J. Am. Chem. Soc.* **2016**, *138*, 3942−3945.
(62) Umapathy, S.; Mallick, B.; Lakshmanna, A. Mode-Dependent Dispersion in Raman Line Shapes: Observation and Implications from Ultrafast Raman Loss Spectroscopy. *J. Chem. Phys.* **2010**, *133*, 024505.
(63) Harbola, U.; Umapathy, S.; Mukamel, S. Loss and Gain Signals in Broadband Stimulated-Raman Spectra: Theoretical Analysis. *Phys. Rev. A: At., Mol., Opt. Phys.* **2013**, *88*, 011801.
(64) Chen, C.; Liu, W.; Baranov, M. S.; Baleeva, N. S.; Yampolsky, I. V.; Zhu, L.; Wang, Y.; Shamir, A.; Solntsev, K. M.; Fang, C. Unveiling Structural Motions of a Highly Fluorescent Superphotoacid by Locking and Fluorinating the GFP Chromophore in Solution. *J. Phys. Chem. Lett.* **2017**, *8*, 5921−5928.
(65) Hoffman, D. P.; Ellis, S. R.; Mathies, R. A. Characterization of a Conical Intersection in a Charge-Transfer Dimer with Two-Dimensional Time-Resolved Stimulated Raman Spectroscopy. *J. Phys. Chem. A* **2014**, *118*, 4955−4965.
(66) Kukura, P.; Frontiera, R.; Mathies, R. A. Direct Observation of Anharmonic Coupling in the Time Domain with Femtosecond Stimulated Raman Scattering. *Phys. Rev. Lett.* **2006**, *96*, 238303.
(67) Frontiera, R. R.; Fang, C.; Dasgupta, J.; Mathies, R. A. Probing Structural Evolution along Multidimensional Reaction Coordinates with Femtosecond Stimulated Raman Spectroscopy. *Phys. Chem. Chem. Phys.* **2012**, *14*, 405−414.
(68) Johnson, P. J. M.; Halpin, A.; Morizumi, T.; Prokhorenko, V. I.; Ernst, O. P.; Miller, R. J. D. Local Vibrational Coherences Drive the Primary Photochemistry of Vision. *Nat. Chem.* **2015**, *7*, 980−986.
(69) Chattoraj, M.; King, B. A.; Bublitz, G. U.; Boxer, S. G. Ultra-Fast Excited State Dynamics in Green Fluorescent Protein: Multiple States and Proton Transfer. *Proc. Natl. Acad. Sci. U. S. A.* **1996**, *93*, 8362−8367.
(70) Brejc, K.; Sixma, T. K.; Kitts, P. A.; Kain, S. R.; Tsien, R. Y.; Ormö, M.; Remington, S. J. Structural Basis for Dual Excitation and Photoisomerization of the *Aequorea victoria* Green Fluorescent Protein. *Proc. Natl. Acad. Sci. U. S. A.* **1997**, *94*, 2306−2311.
(71) Zhao, Y.; Araki, S.; Wu, J.; Teramoto, T.; Chang, Y.-F.; Nakano, M.; Abdelfattah, A. S.; Fujiwara, M.; Ishihara, T.; Nagai, T.; et al. An Expanded Palette of Genetically Encoded Ca^{2+} Indicators. *Science* **2011**, *333*, 1888−1891.
(72) Tang, L.; Wang, Y.; Liu, W.; Zhao, Y.; Campbell, R. E.; Fang, C. Illuminating Photochemistry of an Excitation Ratiometric Fluorescent Protein Calcium Biosensor. *J. Phys. Chem. B* **2017**, *121*, 3016−3023.
(73) Frisch, M. J.; Trucks, G. W.; Schlegel, H. B.; Scuseria, G. E.; Robb, M. A.; Cheeseman, J. R.; Scalmani, G.; Barone, V.; Mennucci, B.; Petersson, G. A.; et al. *Gaussian 09*, revision B.1; Gaussian, Inc.: Wallingford, CT, 2009.
(74) Hochstrasser, R. M. Two-Dimensional Spectroscopy at Infrared and Optical Frequencies. *Proc. Natl. Acad. Sci. U. S. A.* **2007**, *104*, 14190−14196.
(75) Leiderman, P.; Genosar, L.; Huppert, D. Excited-State Proton Transfer: Indication of Three Steps in the Dissociation and Recombination Process. *J. Phys. Chem. A* **2005**, *109*, 5965−5977.
(76) Baranov, M. S.; Lukyanov, K. A.; Borissova, A. O.; Shamir, J.; Kosenkov, D.; Slipchenko, L. V.; Tolbert, L. M.; Yampolsky, I. V.; Solntsev, K. M. Conformationally Locked Chromophores as Models of Excited-State Proton Transfer in Fluorescent Proteins. *J. Am. Chem. Soc.* **2012**, *134*, 6025−6032.
(77) Simkovitch, R.; Karton-Lifshin, N.; Shomer, S.; Shabat, D.; Huppert, D. Ultrafast Excited-State Proton Transfer to the Solvent Occurs on a Hundred-Femtosecond Time-Scale. *J. Phys. Chem. A* **2013**, *117*, 3405−3413.
(78) Peeler, J. C.; Mehl, R. A. Site-Specific Incorporation of Unnatural Amino Acids as Probes for Protein Conformational Changes. In *Unnatural Amino Acids: Methods and Protocols*; Pollegioni, L., Servi, S., Eds.; Humana Press: New York, 2012; pp 125−134.
(79) Arpin, P. C.; Turner, D. B.; McClure, S. D.; Jumper, C. C.; Mirkovic, T.; Challa, J. R.; Lee, J.; Teng, C. Y.; Green, B. R.; Wilk, K. E.; et al. Spectroscopic Studies of Cryptophyte Light Harvesting Proteins: Vibrations and Coherent Oscillations. *J. Phys. Chem. B* **2015**, *119*, 10025−10034.
(80) Wang, Y.; Tang, L.; Liu, W.; Zhao, Y.; Oscar, B. G.; Campbell, R. E.; Fang, C. Excited State Structural Events of a Dual-Emission Fluorescent Protein Biosensor for Ca^{2+} Imaging Studied by Femtosecond Stimulated Raman Spectroscopy. *J. Phys. Chem. B* **2015**, *119*, 2204−2218.
(81) Frank, J. New Opportunities Created by Single-Particle Cryo-EM: The Mapping of Conformational Space. *Biochemistry* **2018**, *57*, 888−888.
(82) Lee, J.; Challa, J. R.; McCamant, D. W. Ultraviolet Light Makes dGMP Floppy: Femtosecond Stimulated Raman Spectroscopy of 2′-Deoxyguanosine 5′-Monophosphate. *J. Phys. Chem. B* **2017**, *121*, 4722−4732.
(83) Hall, C. R.; Conyard, J.; Heisler, I. A.; Jones, G.; Frost, J.; Browne, W. R.; Feringa, B. L.; Meech, S. R. Ultrafast Dynamics in Light-Driven Molecular Rotary Motors Probed by Femtosecond Stimulated Raman Spectroscopy. *J. Am. Chem. Soc.* **2017**, *139*, 7408−7414.

DOI: 10.1021/acs.jpclett.8b00373
J. Phys. Chem. Lett. 2018, 9, 3253−3263